Article

SETTLING VELOCITY AND POLLINATION DYNAMICS IN *DIARRHENA OBOVATA*, A GRASS OF TEMPERATE FOREST EDGES AND UNDERSTORIES

Phillip C. Klahs*

Department of Ecology, Evolution, and Organismal Biology, Iowa State University, Ames, Iowa 50011 USA

Journal of Pollination Ecology, 32(8), 2022, pp 73-86

DOI: 10.26786/1920-7603(2022)683

Received 20 December 2021, accepted 3 June 2022

*Corresponding author: phil.klahs@gmail.com

Abstract—Pollen from a naturally occurring population of the forest grass species *Diarrhena obovata* was successfully captured in a series of pollen traps to understand the timing of anthesis and the dispersal mechanics of wind pollination in an example of the flowering plant family Poaceae. Scanning electron microscopy was used to identify the pollen surface ornamentation as microechinate-areolate. The spherical grains have a diameter of 38.74 µm. The settling velocity calculated by Stoke's Law was 4.48 cm s^{-1}, but physical measurement by drop tower experiments resulted in 3.77 ± 0.15 cm s^{-1} (sd). The surface ornamentation observed in *D. obovata* pollen is not expected to alter drag forces considerably but the reduction of settling velocity may be a result of species-specific pollen grain density. In forest grasses an improvement in settling velocity may be adaptive in overcoming dispersal constraints in an environment where trees obstruct wind speeds and create more turbulence.

Keywords—Settling Velocity, Terminal Velocity, Poaceae, Pollen, Anemophily

INTRODUCTION

Anemophilous plants have evolved reproductive structures under aerodynamic selection that enable the dispersal of pollen by wind (Niklas 1985; Culley et al. 2002; Dafni et al. 2005; Friedman & Barrett 2009; Timerman & Barrett 2021). Although this strategy represents a small percentage (~10%) of seed plant species (Ackerman 2000), this group has outsized contributions to ecological systems (Faegri & van der Pijl 1966). Anemophilous plants, such as Fagaceae and Juglandaceae in temperate forests, Pinaceae and Cupressaceae in the boreal forests, or Poaceae and Cyperaceae in prairies, grasslands, and wetlands, are often dominant in their respective ecosystems (Di-Giovanni et al. 1996; Strömberg 2011; Linder et al. 2018). Sexual reproduction in these critical species depends on pollen release, pollen dispersal by wind, and pollen capture (Niklas 1985, Di-Giovanni & Kevan 1991, Timerman & Barrett 2021). Anemophilous plants can retain their pollen, and often wait until certain environmental conditions are detected before anthesis begins (Faegri & van der Pijl 1966; Whitehead 1969; Subba Reddi et al. 2010). A successful flight towards a conspecific is determined by the interactions of air currents with the physical properties (i.e. size, density, surface morphology) of the pollen grains (Di-Giovanni et al.1989; Culley et al. 2002; Chamecki et al. 2007). Airborne dispersal is possible because of low settling velocities of anemophilous pollen grains (Fuchs 1964; Gregory 1973). Capture of airborne pollen by female reproductive structures requires trajectories of pollen to be unhindered by the wake of air currents around the female parts and synflorescence structures (Niklas 1982; Roussy & Kevan 2000; Harder et al. 2004). Aneomophilous flower aerodynamics in combination with species specific settling velocities of pollen may act as a filter to find conspecifics (Linder & Midgely 1996). Describing anemophily involves a chaotic wind component, but many important biological attributes of this pollination syndrome are quantifiable.

The speciose grass family Poaceae provides an accessible system to study wind pollination, because it has cosmopolitan distribution and exhibits extensive diversity in reproductive morphology (Friedman & Harder 2005; Kellogg 2015; Soreng et al. 2015). Poaceae is ecologically important as a natural component of grasslands and savannahs (Kevan & Tikhmenev 1996), economically important for producing the majority of calories consumed by the global human population (Awika 2011), and a factor in human health as the primary source of pollen allergens (Andersson & Lidholm 2003). Anthesis, in the grasses studied, includes the release of pollen for a few hours each day, and is completed over several successive days (Jones & Newell 1946; Ogden et al. 1969; Subba Reddi et al. 1988, Friedman & Barrett 2008). After crossing some threshold in temperature (Jones & Newall 1946), humidity (Leighty & Sando 1924; Matsui et al. 1999), physical stimulus (Timerman et al. 2014), or other environmental cue (Subba Reddi et al. 2010), the locule wall of the anther splits, opening the way for pollen to be released (Keijzer et al. 1996). Most grass species have pollen with diameters between 20 and 40 μm, an absence of pollenkitt, minimal surface features, and a single pore (Wodehouse 1935; Rempe 1937; Whitehead 1969; Crane 1986; Paw U & Hotton 1989). Exceptions in Poaceae exist, with the pollen of some forest grasses having conspicuous microscopic surface ornamentation (Dórea et al. 2017; Dórea et al. 2018) and the pollen diameters of some domesticated crops, like *Zea mays* L., exceeding the usual size for wind pollinated plants (Aylor 2002). Surprisingly, pollen settling velocity from only a limited sample of grass species have been measured (Durham 1946; Di-Giovanni et al. 1995; Aylor 2002; Borrell 2012, Chamecki et al. 2011), and all are open habitat, weedy or forage or lawn grasses. Measuring the settling velocity of pollen from a forest grass presents information about wind pollination in important forest habitats that has been previously unexplored.

Diarrhena obovata (Gleason) Brandenburg is a perennial grass in the subfamily Pooideae. Commonly known as "beak grass" for the distinctive shape of its seed grain, this grass occurs in forests and along forest edges of mid to eastern North America (Barkworth et al. 1993). At maturity the plants consist of erect culms (48-131 cm) and several dark green, lustrous leaves (6-18 mm wide, 24-72 cm long) (Fig. 1). Spikelets are

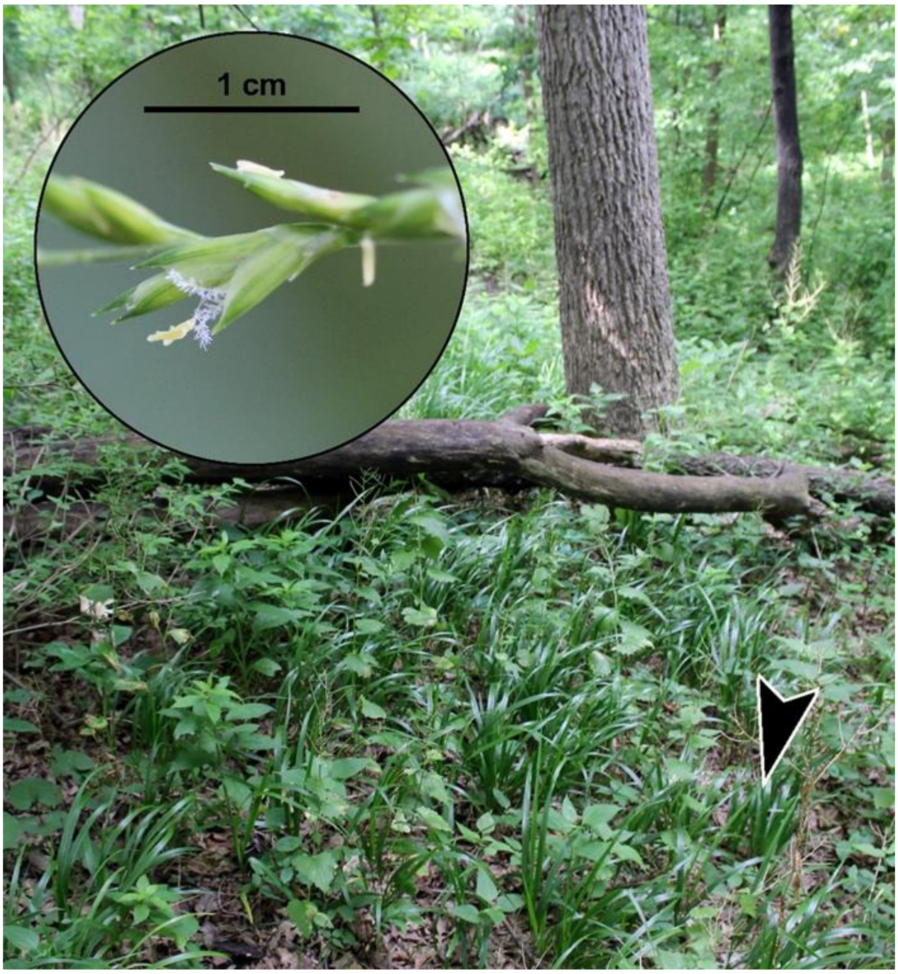

Figure 1. A slope of deciduous forest in Ames, IA with plants of *Diarrhena obovata* indicated by an arrowhead and a view of spikelets shown in the inset.

borne in slender, terminal panicles and are composed of 2 glumes subtending 3 to 5 fertile florets with a rudimentary floret at the apex (Pohl 1966). Although many aspects of the morphology of this species were documented by Schwab (1971), the surface ornamentation and settling velocity of *D. obovata* pollen are not yet known.

There are a variety of ways to study pollination dynamics, with some modern methods of measuring settling velocity utilizing sophisticated technology (van Hout & Katz 2004, Friedman & Harder 2004, Dafni et al. 2005; Loubet et al. 2007; Hirose & Osada 2016), and many techniques of pollen trapping relying on sets of expensive equipment (Raynor et al.1972; Linder & Midgley 1996; Di-Giovanni et al. 1996; Dafni et al. 2005; Subba Reddi et al. 2010). The methods implemented in this study were chosen under unusual circumstances with limited financial resources during the summer of 2020, but provide an example of relatively simple scientific methods that still answer technical questions. Timing the descent of pollen through a known distance of still air in a cardboard tube, such as I used here, may even have advantages over metal drop tower apparatuses that can introduce electrical charges (McCubbin 1918; Dyakowska 1937; Durham 1946; Di-Giovanni et al. 1995). The aims of my study were to 1) document and quantify grass pollen release in a naturally occurring population of the forest species *D. obovata*; 2) observe the surface ornamentation of the pollen with scanning electron microscopy; 3) measure the pollen diameter to calculate a predicted settling velocity; 4) measure settling velocity of the pollen with drop tower experiments; and 5) compare the predicted and measured settling velocities with each other, as well as other published values in the literature. These results contribute to an understanding of how a forest grass accomplishes pollination and provide new data for the comparative reproductive biology of grass pollen dispersal.

MATERIALS AND METHODS

FIELD STUDY

A naturally occurring population of *D. obovata* growing on the northwest corner of Iowa State University's (ISU) campus (N 42° 1' 55.4084" W 93° 39' 9.8233") in the ~14-hectare mixed deciduous forest known as Pammel Woods (Norris 1995) was used for this study. Wind moves through this space primarily from east to west and was measured with anemometers in the field. The Ada Hayden Herbarium (ISC) contains local specimens of *D. obovata* with records of anthesis occurring during the month of July. Preliminary collecting trips were made in the growing seasons of 2017 and 2018 to confirm the location of plants and the approximate dates of anthesis. Seeds were collected during these trips, and in the spring of 2018 and 2019 seeds were germinated and grown in the Pohl Conservatory greenhouse at ISU. The plants in the greenhouse and those growing naturally in the field study site were monitored throughout the entire 2020 growing season for signs of flowering and anthesis. The population of *D. obovata* in the field study site was mapped (Fig. 2), and individuals were counted during the fall of 2020 by walking parallel transects and systematically spray painting the base of each culm to avoid skipping or recounting individuals. This process was aided by satellite images (Google Maps 2020) and open-source elevation data (Richardson & Camper 2019).

Pollen traps were made from glass microscope slides (25 x 75 x 1 mm) with petroleum jelly on one surface similar to the method used by Jones (1952). The pollen traps were held in a 1.5 cm deep cut on the top of wooden stakes at a 15° angle. Slides were exposed approximately a meter from the surface of the ground to mimic the location of spikelets on mature culms of *D. obovata*. Slides were manually collected and replaced at approximately 24 to 48 hour intervals from 1 July 2020 until 20 July 2020. The stations were identified by letters "A" through "U" in sequential order along the path walked while making a collection (Fig. 2), and collection numbers began when grass flowers began blooming. Some pollen trap slides were considered contaminated and removed before analyses, including four pollen trap slides that fell from their stations during their exposure (A2, an early station P, P2, and P4) and one slide that was dropped while it was being transferred to the slide box (S6).

Pollen trap slides were observed under a Nikon Eclipse 55i light microscope (nikonmetrology.com) at 100× magnification. Pollen grains per cm^2 were obtained by counting *D. obovata* pollen and dividing by the area viewed (2.97 cm^2). The rate of pollen deposition was calculated by dividing

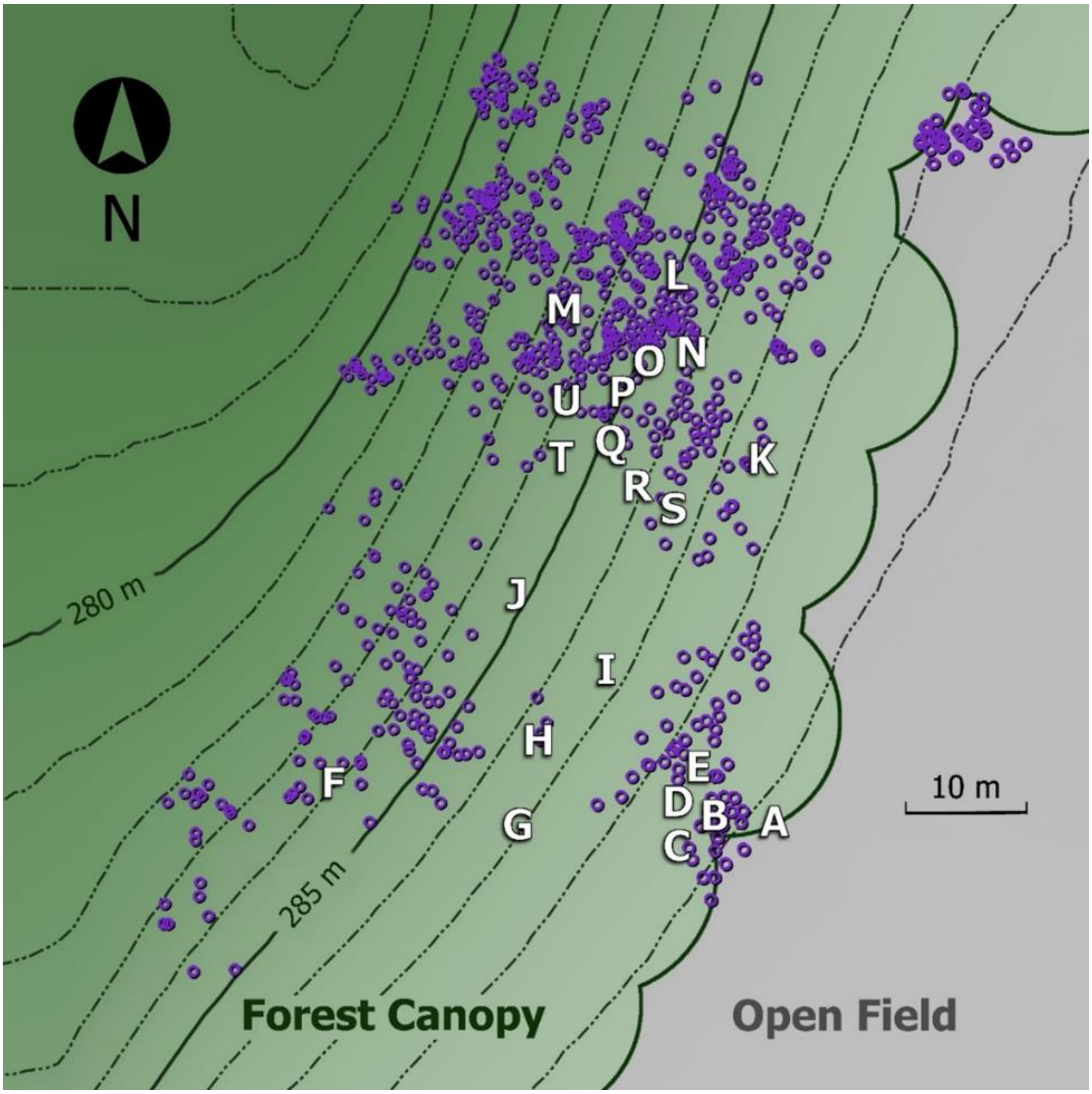

Figure 2. Map of the study site within Pammel Woods from N 42° 1' 55.0642" to N 42° 1' 51.5928" and W 93° 39' 7.7369" to W 93° 39' 14.6477" with elevation and scale denoted. Mature culms of *D. obovata* are indicated by purple rings and pollen trap stations are labelled with white letters. Forest canopy is represented with a green layer, while open canopy of the adjacent field is colored grey.

pollen per cm^2 by the duration in hours of exposure. The kernel density of captured pollen with respect to time was used to determine the peaks of anthesis and was calculated with the 'sm' package in R statistical language (Bowman & Azzalini 2019) separately for three values of smoothing bandwidths (10, 15, and 20).

Climatic data of temperature, wind speed, and wind direction at 15-minute intervals were obtained from an existing weather station on the roof of a university building less than 200 m away from the field study site. Temperature data was grouped into 12-hour nocturnal and diurnal segments separated by 6 am and 6 pm. Precipitation data was obtained from the records of a weather station at the Ames Municipal Airport and divided into 24-hour segments.

POLLEN CHARACTERISTICS

Pollen grains collected from greenhouse plants were stored in a glass jar with a canning lid and used as a supply of pollen grains for the subsequent procedures. A small amount of pollen was provided to the Roy J. Carver High Resolution

Microscopy Facility at Iowa State University and deposited onto conductive backed adhesive tape on an aluminum stub and sputter coated with platinum using a Cressington HR208 high resolution sputter coater (tedpella.com). Images of the surface ultrastructure were captured at 2000×, 5000×, and 10000× magnifications using a Hitachi SU4800 field emission scanning electron microscope (hitachi-hightech.com).

The diameters of 98 pollen grains were measured using an ocular micrometer at 200× magnification with a Nikon Eclipse 55i light microscope (nikonmetrology.com) and converted into millimeters. The mean particle diameter was used to predict the settling velocity (m s^{-1}) by calculating the Stokes' law equation (Stokes 1901; DiGiovanni et al. 1995).

$$V_{set} = \frac{2gr^2(\rho_p - \rho_a)}{9\mu}$$

At an air temperature of 20°C this equation uses the variable g for the acceleration of gravity (9.8 m s^{-2}), ρ_a for the density of the air (1.204×10^{-3} kg m^{-3}), and μ for the dynamic viscosity of air (1.825×10^{-5} kg m^{-1} s^{-1}) (Riest 1984). The variable r is the radius in meters of a spherical particle, and ρ_p is the particle density (kg m^{-3}). In this study the density of grass pollen was assumed to be 1000 kg m^{-3}, which is equivalent to 1 g cm^{-3}. This method of predicting settling velocity also relies on the assumption that the pollen grains have a sufficiently low Reynolds number. Small, spherical particles with a Reynolds number < 1 have laminar flow that permits the Stoke's law equation, but if that assumption is violated and the particle is large enough to produce turbulent flow it becomes a system not accurately described by Stoke's law (DiGiovanni et al. 1995). The investigation of surface features, in combination with the diameter measurements, was conducted to assess potential excessive drag forces that would prevent Stoke's law from applying.

A drop tower apparatus was constructed from an inner cardboard tube with a diameter of 5.3 cm and an outer cardboard tube with a diameter of 7.5 cm (McCubbin 1918; Gregory 1945; Ferrandino & Aylor 1984). The tower was 150 cm tall and had a basal aperture of 1 cm^2. Following the procedures of Borrell (2012), the head of an electric toothbrush was used to introduce particles at the top of the drop tower. A series of microscope slides with petroleum jelly captured pollen beneath the basal aperture in four second intervals as the slides were manually progressed. Pollen captured by each slide was later observed with a light microscope, counted, and assigned a time of descent based on the midpoint of the four second intervals. Eight trials of drop tower experiments were conducted, but the first three were discarded because an insufficient amount of pollen was used. All trials were conducted at 19 °C and 36% humidity with low wind circulation in the room. Kernel density curves were calculated for pollen descent times by trial (Bowman & Azzalini 2019), and the maxima of these curves were taken to be the respective time of descent for average *D. obovata* pollen grains. Settling velocity was calculated for each trial as the ratio of distance the pollen travelled (150 cm) over the time of descent. A one-tailed Student's t-test was conducted to determine if the settling velocity measured by the drop tower experiments was significantly lower than the settling velocity predicted by the Stokes' law. In an effort to improve the resolution of this study the initiation of slide progressions of some trials was offset by 1, 2, or 3 seconds. An analysis of variance was conducted on the descent times of pollen in trials used to calculate the overall settling velocity to determine if a difference in measured settling velocity existed between the offset treatments.

RESULTS

FIELD STUDY

The population of *Diarrhena obovata* studied during the growing season of 2020 consisted of 837 culms. In total 136 slides were exposed to potentially catch pollen during the field portion of this study. Pollen of *D. obovata* was recorded on 38 of the 136 pollen trap slides (Tab.1). The duration of anthesis in *D. obovata* was demarcated by the presence of pollen in the atmosphere between July 8 and July 17, and this timeframe is highlighted in Fig. 3. Diurnal and nocturnal temperatures fluctuated during the anthesis period but three distinct declines in temperature were recorded in this window of time (see July 9, 11, and 15 in Fig. 3B). The first and second declines in temperature were abrupt, happening within 24 hours, but the third was a gradual decline over several days. Declining temperatures on the night of July 11 and

Table 1. Pollen grains of *D. obovata* collected by pollen traps in Pammel Woods, Ames, IA in July 2020. (Continued next page)

		Collected July 9				Collected July 10				Collected July 11			
Station	Distance from Pop. Center (m)	Pollen Grains	Grains per cm2	Duration (hrs.)	Accumulation Rate	Pollen Grains	Grains per cm2	Duration (hrs.)	Accumulation Rate	Pollen Grains	Grains per cm2	Duration (hrs.)	Accumulation Rate
A	3.05*	0	0	40	0	0	0	24	0	0	0	24	0
B	1.5	26	8.75	40	0.219	198	66.67	24	2.778	2	0.67	24	0.028
C	3.05	0	0	40	0	0	0	24	0	1	0.34	24	0.014
D	3.05	16	5.39	40	0.135	101	34.01	24	1.417	0	0	24	0
E	3.05	8	2.69	40	0.067	29	9.76	24	0.407	0	0	24	0
F	17.37	0	0	40	0	-	-	-	-	0	0	48	0
G	9.75	0	0	40	0	-	-	-	-	3	1.01	48	0.021
H	9.45	0	0	40	0	-	-	-	-	3	1.01	48	0.021
I	9.75	0	0	40	0	-	-	-	-	2	0.67	48	0.014
J	15.25	0	0	40	0	-	-	-	-	0	0	48	0
K	6.10*	0	0	40	0	-	-	-	-	0	0	48	0
L	7.62	0	0	40	0	-	-	-	-	0	0	48	0
M	9.75	0	0	40	0	-	-	-	-	0	0	48	0
N	7.62	0	0	40	0	-	-	-	-	7	2.36	48	0.049
O	3.66	0	0	40	0	1	0.34	24	0.014	3	1.01	24	0.042
P	3.66	0	0	40	0	0	0	24	0	0	0	24	0
Q	3.66	1	0.33	40	0.008	2	0.67	24	0.028	2	0.67	24	0.028
R	3.66	0	0	40	0	13	4.38	24	0.182	6	2.02	24	0.084
S	3.66	0	0	40	0	-	-	-	-	1	0.34	48	0.007
T	6.71	0	0	40	0	-	-	-	-	2	0.67	48	0.014
U	7.62	0	0	40	0	-	-	-	-	0	0	48	0

the separate decline leading into the day of July 16 were both accompanied by precipitation events with a small amount of rain on July 12 and a large thunderstorm on July 15 to 16 (Fig. 3C). Pollen traps recorded a major decline in airborne pollen around both periods of precipitation. An additional 20 pollen trap slides not included in Tab.1 recorded the absence of any *D. obovata* pollen for 130 hours preceding the first numbered collection on July 9 and for 65 hours following the collection on July 17.

For each slide the total pollen grains captured, the density of pollen grains per cm^2, the duration of trap exposure, and the resulting accumulation rate are provided in Tab.1. The highest rate of accumulation (2.78 grains per cm^2 per h) was measured by station "B" on July 10. Anthesis was determined by maxima of kernel density calculations to peak July 9-10 followed by a second, weaker peak on July 14 (Fig. 3A). These peaks occurred during periods of warm weather (Fig. 3B) separated by lower temperatures on the night of July 11 and 0.36 inches of precipitation on July 12 (Fig. 3C). Slides that recorded no captured pollen were quite common, with 72% of pollen traps exposed during anthesis having no grains of *D. obovata* observed in the 2.97 cm^2 viewed. Success of stations, however, was relatively high as 16 of the 21 stations captured at least one pollen grain during the course of this study.

Table 1. continued. Station distances marked with * were east of the population center and considered upwind.

		Collected July 12				Collected July 13				Collected July 13			
Station	Distance from Pop. Center (m)	Pollen Grains	Grains per cm2	Duration (hrs.)	Accumulation Rate	Pollen Grains	Grains per cm2	Duration (hrs.)	Accumulation Rate	Pollen Grains	Grains per cm2	Duration (hrs.)	Accumulation Rate
A	3.05*	3	1.01	32	0.032	0	0	16	0	-	-	-	-
B	1.5	3	1.01	32	0.032	51	17.17	16	1.073	1	0.34	55.5	0.006
C	3.05	2	0.67	32	0.021	7	2.35	16	0.147	-	-	-	-
D	3.05	2	0.67	32	0.021	20	6.73	16	0.421	-	-	-	-
E	3.05	0	0	32	0	30	10.1	16	0.631	-	-	-	-
F	17.37	0	0	32	0	0	0	16	0	-	-	-	-
G	9.75	0	0	32	0	3	1.01	16	0.063	-	-	-	-
H	9.45	-	-	-	-	3	1.01	48	0.021	-	-	-	-
I	9.75	-	-	-	-	4	1.34	48	0.028	0	0	55.5	0
J	15.25	-	-	-	-	1	0.33	48	0.007	-	-	-	-
K	6.10*	0	0	32	0	0	0	48	0	-	-	-	-
L	7.62	0	0	32	0	0	0	48	0	-	-	-	-
M	9.75	-	-	-	-	0	0	48	0	-	-	-	-
N	7.62	-	-	-	-	3	1.01	48	0.021	0	0	55.5	0
O	3.66	2	0.67	32	0.021	0	0	16	0	-	-	-	-
P	3.66	0	0	32	0	0	0	16	0	0	0	55.5	0
Q	3.66	0	0	32	0	0	0	16	0	-	-	-	-
R	3.66	0	0	32	0	7	2.35	16	0.147	-	-	-	-
S	3.66	-	-	-	-	1	0.33	48	0.007	-	-	-	-
T	6.71	-	-	-	-	0	0	48	0	-	-	-	-
U	7.62	-	-	-	-	0	0	48	0	-	-	-	-

POLLEN CHARACTERISTICS

The pollen of *D. obovata* consisted primarily of spherical monads having a mean diameter of 38.74 µm (*N* = 98, sd = 2.94) with some deformation occurring as the result of desiccation. A single porate aperture, with an annulus (Fig. 4A, arrow) and an operculum (Fig. 4B, arrow) was visible at 200× magnification with light microscopy and imaged at 2000× and 5000× magnification using scanning electron microscopy (Fig. 4A, B). According to Dórea et al. (2017; 2018), the ectexine surface would be classified as "microechinate-areolate", characterized by microspines protruding from raised polygonal areolas (Fig. 4B, C).

Although the Reynolds number was not explicitly tested, the surface features observed with SEM and the average diameter indicate the pollen of *D. obovata* should have a low enough Reynolds number to appropriately use the Stoke's law. For a particle of this shape and size Stoke's law predicts a settling velocity of 4.48 cm s^{-1}. Five trials of drop tower experiments captured sufficient amounts of pollen (Tab.2) and measured reasonable distributions of descent times. The kernel density of pollen descent times for these trials was calculated and plotted in Fig. 5. The maximum value at the inflection point of each curve was taken as the peak deposition time for the

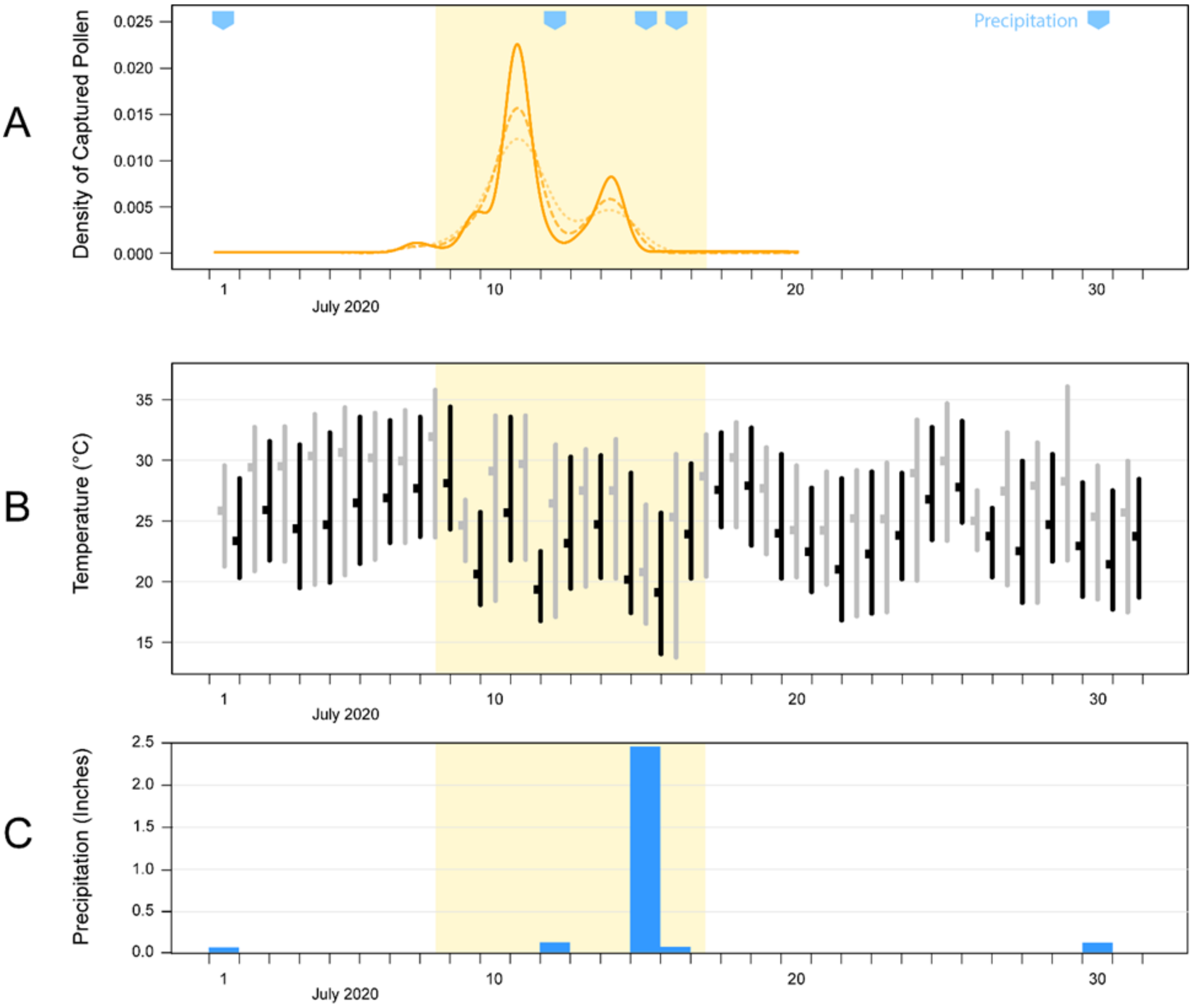

Figure 3. Timeline of July 2020 with A) kernel densities of captured pollen using three smoothing bandwidths of 10 (solid line), 15 (dashed line), and 20 (dotted line), B) temperature ranges in Celsius of diurnal (grey lines) and nocturnal (black lines) 12-hour periods with the mean indicated as an adjacent box, and C) precipitation in inches. The yellow band highlights the period of anthesis measured for *D. obovata*.

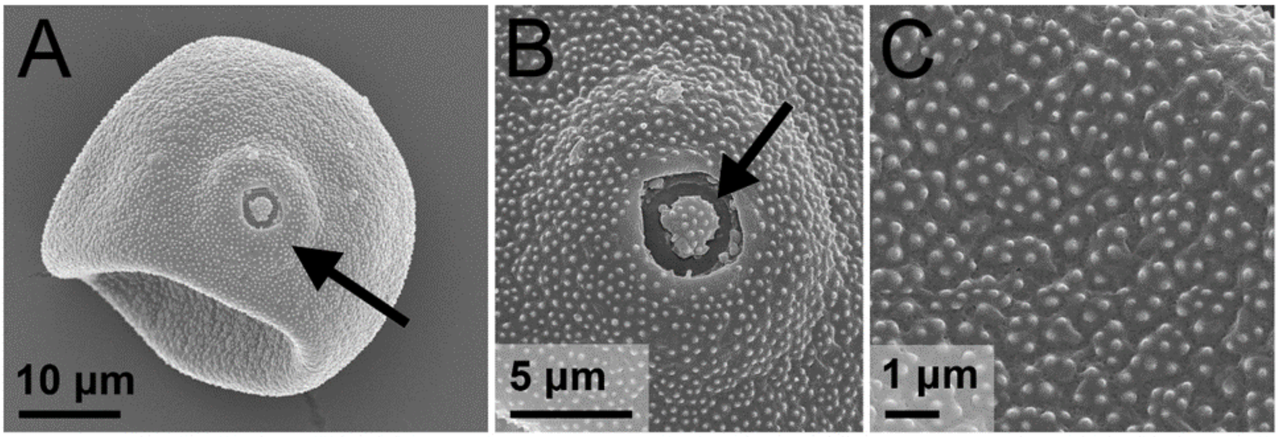

Figure 4. View of *D. obovata* pollen surface under SEM at A) 2000× B) 5000× C) 10000× magnifications. Arrows indicate the annulus in A and the operculum in B.

Table 2. Number of *D. obovata* pollen grains captured at the bottom of 1.5 m drop tower during time intervals after pollen release.

Trial 4		Trial 5		Trial 6		Trial 7		Trial 8	
Time (seconds)	Pollen Captured	Time (seconds)	Pollen Captured	Time (seconds)	Pollen Captured	Time (seconds)	Pollen Captured	Time (seconds)	Pollen Captured
25-29	0	25-29	0	26-30	0	26-30	0	27-31	0
29-33	1	29-33	5	30-34	2	30-34	3	31-35	3
33-37	1	33-37	31	34-38	12	34-38	29	35-39	25
37-41	5	37-41	33	38-42	31	38-42	31	39-43	14
41-45	3	41-45	26	42-46	7	42-46	3	43-47	19
45-49	3	45-49	4	46-50	4	46-50	5	47-51	3
49-53	1	49-53	5	50-54	0	50-54	2	51-55	4
53-57	1	53-57	0	54-58	0	54-58	0	55-59	0

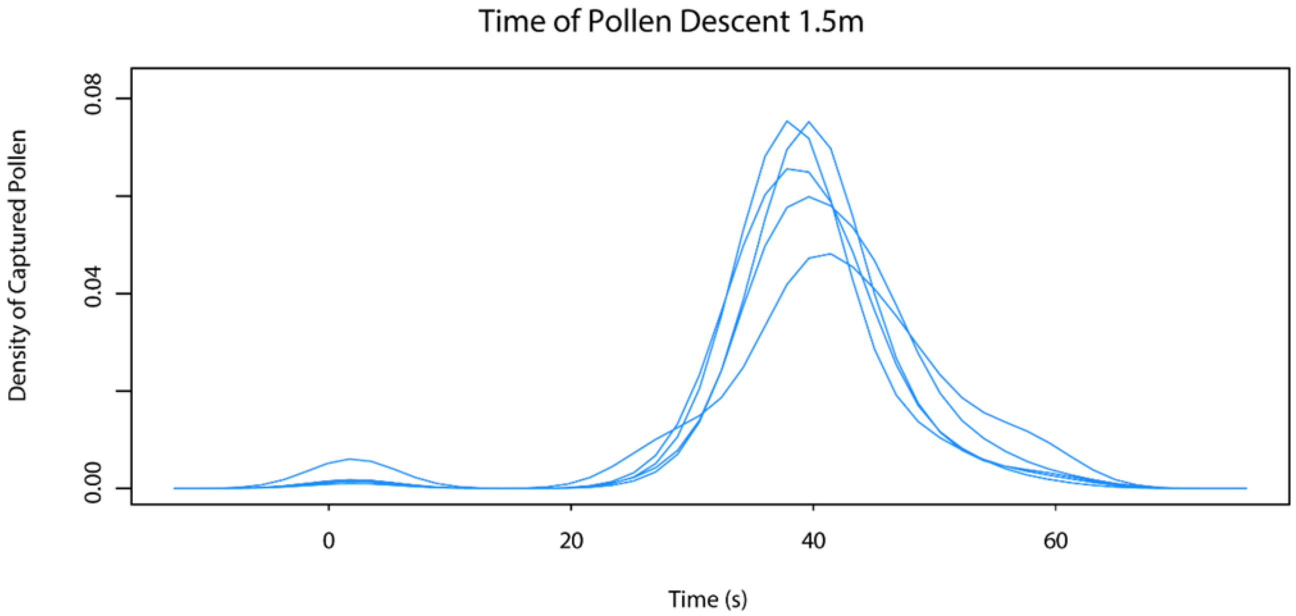

Figure 5. The kernel density plots of *D. obovata* pollen grains captured per slide for the five trials measuring descent times 1.5 m through still air in a drop tower.

corresponding trial, which used in a ratio with the distance travelled (1.5 m) recorded settling velocities (cm s^{-1}) of 3.56, 3.87, 3.79, 3.93, and 3.69 ($\bar{x} = 3.77$, sd = 0.15).

The experimentally measured settling velocity was determined to be significantly less than the value predicted by the Stoke's law equation by the statistical rejection of the null hypothesis for a one tailed Student's t-test ($P < 0.005$, df = 4). Conversely,

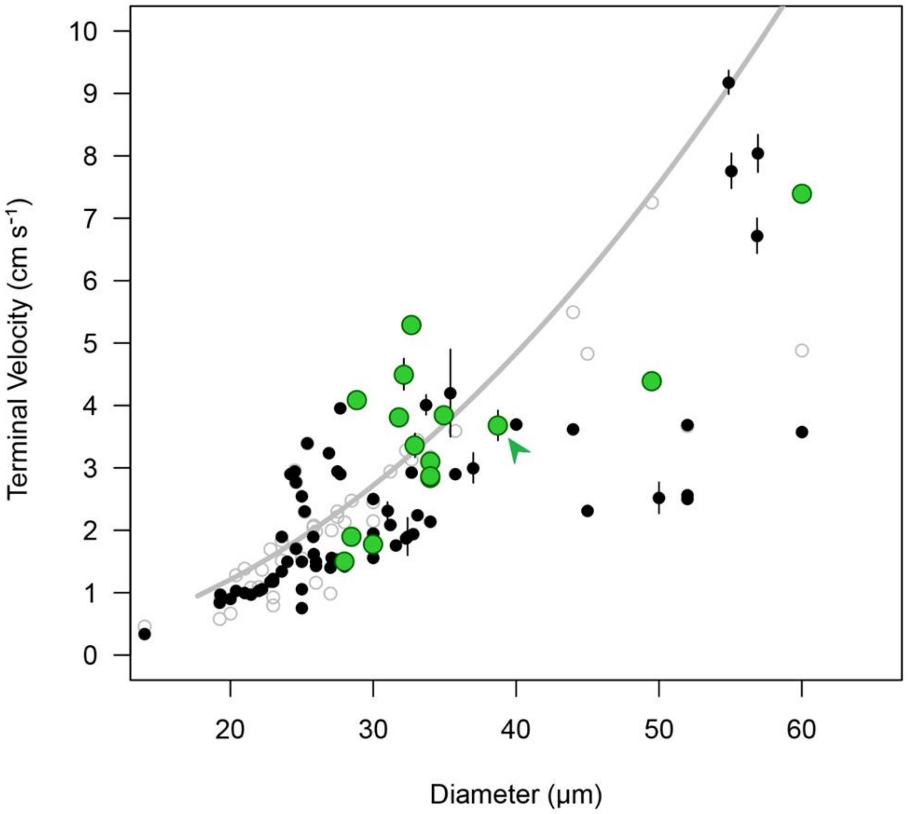

Figure 6. Settling velocities of angiosperm pollen grains either published in the literature (green dots are Poaceae, black dots are other families) or estimated from published diameters and densities (empty grey circles). The grey line indicates settling velocity values predicted by the Stokes' law when density is assumed to be 1 kg m-3 for a range of diameters. The green arrow indicates the settling velocity of *D. obovata* measured in this study.

the inability to reject the null hypothesis in a one-way analysis of variance indicated no significant difference between trials offset to improve resolution and the group mean ($F = 1.66$, df = 2). A comparison to other reported measurements of settling velocity and theoretical values in the literature is provided in Fig. 6. This graph includes only pollen of angiosperms (Dahl & Ellis 1942; Durham 1946; Di-Giovanni et al. 1995; Duffin & Bunting 2008; Sosnoskie et al. 2009; Borrell 2012; Ecker et al. 2013) to avoid comparisons with the pollen of conifers that may have air bladder appendages. Estimates were also calculated from published diameters and densities of Poaceae pollen grains (Jones 1952; Joly et al. 2007; Mitsumoto et al. 2009; Radaeski et al. 2016) using the same air temperature and dynamic viscosities as before from Riest (1984). The pollen diameters, densities, measured settling velocities, and calculated settling velocities used to produce Fig. 6 are also included as a supplemental table.

DISCUSSION

ANTHESIS

The *Diarrhena obovata* population documented in this study experienced conditions not ideal for pollen dispersal during anthesis in 2020. The challenge of capturing pollen to document that window of anthesis was increased by turbulent wind patterns, sloping environment, and low density of individuals. These impediments to sustained airborne pollen are real conditions that are regularly overcome by anemophilous forest understory plants. Studying wind pollinated plants in a natural system provides perspective for the chaotic nature of wind pollination and the selective forces shaping anemophilous reproduction.

Precipitation reduced the amount of airborne pollen grains recorded by this study (Fig. 3). The data collected during this field study measured pollen deposition at stations and does not reflect the amount of pollen released. It is possible that *D. obovata* began dehiscing pollen on July 8 and proceeded with a continuous rate of dehiscence until supplies were depleted. The reduction of captured pollen could be because rain effectively removed pollen from the air, or from an arresting mechanism. Days with precipitation were preceded by nights of low temperatures which may have slowed separation between pollen and the tapetum in the locule of the anther

(Christensen & Horner 1974). The continuation of anthesis over several days increases the chance of pollen deposition even with intermittent weather events (Fig. 3), as by the end of the study 76% of pollen trap stations were "pollinated".

POLLEN CHARACTERISTICS

The pollen grains exhibit surface characteristics of the microechinate-areolate pollen type which is reported as common and has been found in distantly related tribes of Poaceae (Dórea et al. 2017). It has been suggested by Rempe (1937) that the ultrastructure of pollen can create additional drag or can accumulate a boundary layer of still air that could effectively increase the diameter of the particle without a heavy investment in additional mass. While the microspines observed in this study may interact with air to some degree, the diminutive size of these structures, when compared to other pollen considered to be ornamented, suggests the surface features of *D. obovata* do not significantly impact the aerodynamics of the whole structure.

POLLEN DENSITY

Density, or the specific density, in this instance refers to the mass over volume relationship of the whole pollen grain and not of the organic substances composing the particle (Durham 1943). Measuring this value in small particles is difficult, and complicated in grasses by hollow intra-exinous channels which make the pollen grains compressible (Larson et al. 1962). The density of grass pollen theoretically does not deviate from a value of 0.988 or 1 g cm^{-3} (Durham 1943; Niklas 1985; Paw U & Hotton 1989; DiGiovanni et al. 1995; Borrell 2012). It has become the convention to assume these values in the Stoke's law equation for taxa where the density of pollen grains is unknown. The settling velocity of *D. obovata* pollen measured by drop tower experiments in this study was 15.8% slower than the value predicted by Stoke's law. A smaller pollen density would explain a slower rate of descent. The challenge of measuring the density of such small particles as individual grains of pollen is so great that an alternative route to acquire a working value for the density of pollen has been employed by van Hout & Katz (2004), who experimentally measured the settling velocity of pollen and then worked backwards through the Stoke's law equation to predict density. Conducting this reverse procedure with settling velocity data obtained from this study would predict a density of 0.8 g cm^{-3} for pollen grains of *D. obovata*. The density also does not remain constant as desiccation is known to reduce the mass of pollen grains over time (Aylor 2003) and may play a role in extending the dispersal capabilities of anemophilous pollen. As Niklas (1985) noted in his work on aerodynamics of wind pollination, "divergence in spore or pollen morphology from perfectly spherical shapes, and the addition of low-density volumes result in profound differences between theoretical and observed terminal settling velocities".

Physics equations can provide insight into the biomechanical aspects of botanical phenomena and there is utility in predicting the aerodynamic properties of anemophilous pollen, but assumptions may distract from aspects responsible for pollination success. For example, pollen grains of *Diarrhena obovata*, a perennial understory grass, are released mid July, are spherical in shape with a 38.74 μm diameter, have a single pore, and are covered in microechinate-areolate surface ornamentation. Although these attributes are consistent with other pollen in the stenopalynous grass family the grains of *D. obovata* show discrepancies between predicted and observed settling velocities. This study used physical measurements of *D. obovata* pollen grains falling down a still collumn of air to determine a settling velocity of 3.77 cm s^{-1} and represents the first instance of measured pollen settling velocity from a forest grass species. Expanding sampling beyond common, open canopy species or trees to include anemophilous species adapted to life in forest understories may expose assumptions about pollen density and reveal adaptations like species specific pollen settling velocities that enable successful sexual reproduction in chaotic environments.

ACKNOWLEDGEMENTS

The writing of this manuscript was accomplished with advice from Dr. Lynn Clark, Dept. of Ecology, Evolution, and Organismal Biology (EEOB), Iowa State University (ISU). The manuscript was also improved by the help of reviewers. The author would like to extend special thanks to Tracey Stewart of the Roy J. Carver High Resolution Microscopy Facility at ISU for capturing SEM images of pollen and to Sarah Klahs for assisting with the settling velocity experiments. This study was funded by the Harry and Audrey Finch Scholarship in Botany through the Dept. of EEOB.

APPENDICES

Additional supporting information may be found in the online version of this article:

Appendix. A table of previously published settling velocities measured or estimated for angiosperms. Species of Poaceae with published pollen grain diameters are also included and used to calculate a settling velocity estimate with the Stoke's law equation.

REFERENCES

Ackerman JD (2000) Abiotic pollen and pollination: ecological, functional, and evolutionary perspectives. In Pollen and Pollination 167-185 Springer, Vienna.

Andersson K, Lidholm J (2003) Characteristics and immunobiology of grass pollen allergens. International archives of allergy and immunology 130(2): 87-107.

Awika JM (2011) Major cereal grains production and use around the world. In Advances in cereal science: implications to food processing and health promotion (pp. 1-13). American Chemical Society.

Aylor DE (2002) Settling speed of corn (*Zea mays*) pollen. Journal of Aerosol Science 33(11): 1601-1607.

Aylor DE (2003) Rate of dehydration of corn (*Zea mays* L.) pollen in the air. Journal of Experimental Botany 54(391): 2307-2312.

Barkworth ME, Capels KM, Long S (1993) Flora of North America, North of Mexico: Volume 24: Magnoliophyta: Commelinidae (in Part): Poaceae, Part 1 (Vol. 24). Oxford University Press on Demand.

Borrell JS (2012) Rapid assessment protocol for pollen settling velocity: implications for habitat fragmentation. Bioscience Horizons: The International Journal of Student Research, 5.

Bowman A, Azzalini A (2019) Package 'sm'. Version 2.2-5.6 (27 September 2018) http://cran.r-project.org/web/packages/sm (accessed 4 December 2020).

Chamecki M, Van Hout R, Meneveau C, Parlange MB (2007) Concentration profiles of particles settling in the neutral and stratified atmospheric boundary layer. Boundary-layer meteorology 125(1): 25-38.

Chamecki M, Gleicher SC, Dufault NS, Isard SA (2011) Diurnal variation in settling velocity of pollen released from maize and consequences for atmospheric dispersion and cross-pollination. Agricultural and forest meteorology 151(8): 1055-1065.

Christensen JE, Horner HT (1974) Pollen pore development and its spatial orientation during microsporogenesis in the grass Sorghum bicolor. American Journal of Botany 61(6): 604-623.

Crane PR (1986) Form and function in wind dispersed pollen. In Linnean Society symposium series 12: 179-202.

Culley TM, Weller SG, Sakai AK (2002) The evolution of wind pollination in angiosperms. Trends in Ecology and Evolution 17(8): 361-369.

Dafni A, Kevan PG, Husband BC (2005) Practical pollination biology. *Practical pollination biology*.

Dahl AO, Ellis RV (1942) The pollen concentration of the atmosphere. Public Health Reports *(1896-1970)*: 369-377.

Di-Giovanni F, Beckett PM, Flenley JR (1989) Modelling of dispersion and deposition of tree pollen within a forest canopy. *Grana 28*(2): 129-139.

Di-Giovanni F, Kevan PG (1991) Factors affecting pollen dynamics and its importance to pollen contamination: a review. Canadian Journal of Forest Research 21(8): 1155-1170.

Di-Giovanni F, Kevan PG, Nasr ME (1995) The variability in settling velocities of some pollen and spores. Grana 34(1): 39-44.

Di-Giovanni F, Kevan PG, Caron GÉ (1996) Estimating the timing of maximum pollen release from jack pine (Pinus banksiana Lamb.) in northern Ontario. The Forestry Chronicle 72(2): 166-169.

Dórea MDC, de Oliveira RP, Banks H, Dos Santos FDAR (2017) Sculptural elements on the ectexine surface of Poaceae pollen from Neotropical forests: patterns and implications for taxonomic and evolutionary studies in this family. Botanical Journal of the Linnean Society 185(4): 542-571.

Dórea MC, Santos DWJ, Oliveira RP, Funch LS, Santos FAR (2018) Reproductive traits related to anemophily and insect visitors in two species of Poaceae from the Brazilian Atlantic rainforest. Brazilian Journal of Botany 41(2): 425-434.

Duffin KI, Bunting MJ (2008) Relative pollen productivity and fall speed estimates for southern African savanna taxa. Vegetation History and Archaeobotany *17*(5): 507-525.

Durham OC (1943) The volumetric incidence of atmospheric allergens: I. Specific gravity of pollen grains. Journal of Allergy 14(6): 455-461.

Durham OC (1946) The volumetric incidence of atmospheric allergens: III. Rate of fall of pollen grains in still air. Journal of Allergy 17(2): 70-78.

Dyakowska J (1937) Researches on the rapidity of the falling down of pollen of some trees. Bulletin of the Polish Academy of Sciences B. I:155-168.

Ecker G, Meyer T, Auer C (2013) Pollen longevity and dispersion models for switchgrass. Crop Science *53*(3): 1120-1127.

Faegri K, van der Pijl L (1966) The principles of pollination ecology. Toronto and Oxford.

Ferrandino FJ, Aylor DE (1984) Settling speed of clusters of spores. Phytopathology 74(8): 969-972.

Friedman J, Barrett SC (2008) A phylogenetic analysis of the evolution of wind pollination in the angiosperms. International Journal of Plant Sciences 169(1): 49-58.

Friedman J, Barrett SC (2009) Wind of change: new insights on the ecology and evolution of pollination and mating in wind-pollinated plants. Annals of Botany 103(9): 1515-1527.

Friedman J, Harder LD (2004) Inflorescence architecture and wind pollination in six grass species. Functional Ecology, pp.851-860.

Friedman J, Harder LD (2005) Functional associations of floret and inflorescence traits among grass species. American Journal of Botany 92(11): 1862-1870

Fuchs NA (1964) The mechanics of aerosols. New York: Macmillan

Google Maps (2020) Map of Iowa State University. Available at: https://www.google.com/maps/place/Iowa+State+University/ (Accessed: October 2020).

Gregory PH (1945) The dispersion of air-borne spores. Transactions of the British Mycological Society 28(1-2): 26-72.

Gregory PH (1973) The microbiology of the atmosphere. 2nd edition. Leonard Hill, Aylesbury.

Harder LD, Jordan CY, Gross WE, Routley MB (2004) Beyond floricentrism: the pollination function of inflorescences. Plant Species Biology 19(3):137-48.

Hirose Y, Osada K (2016) Terminal settling velocity and physical properties of pollen grains in still air. Aerobiologia 32(3): 385-394.

Joly C, Barillé L, Barreau M, Mancheron A, Visset L (2007) Grain and annulus diameter as criteria for distinguishing pollen grains of cereals from wild grasses. Review of Paleobotany and Palynology 146(1-4): 221-233.

Jones MD, Newell LC (1946) Pollination cycles and pollen dispersal in relation to grass improvement. Bulletin of the Agricultural Experiment Station of Nebraska No. 148

Jones MD (1952) Time of day of pollen shedding of some hay fever plants. Journal of Allergy 23(3): 247-258.

Keijzer CJ, Leferink-ten Klooster HB, Reinders MC (1996) The mechanics of the grass flower: anther dehiscence and pollen shedding in maize. Annals of Botany 78(1): 15-21.

Kellogg EA (2015) Flowering plants. Monocots. Cham: Springer International Publishing DOI 10: 978-3.

Kevan PG, Tikhmenev EA (1996) Dynamic anemophily and the ecology of pollination in common grasses in Ontario. *Russian Journal of Ecology 27*(4): 260-266.

Larson DA, Skvarla JJ, Lewis CW (1962) An electron microscope study of exine stratification and fine structure. Pollen Spores 4(2): 233–246.

Leighty CE, Sando WJ (1924) The blooming of wheat flowers. Journal of Agricultural Research 27: 231-244.

Linder HP, Midgley J (1996) Anemophilous plants select pollen from their own species from the air. Oecologia 108: 85–8.

Linder HP, Lehmann CE, Archibald S, Osborne CP, Richardson DM (2018) Global grass (Poaceae) success underpinned by traits facilitating colonization, persistence and habitat transformation. Biological Reviews 93(2): 1125-1144.

Loubet B, Jarosz N, Saint-Jean S, Huber L (2007) A method for measuring the settling velocity distribution of large biotic particles. Aerobiologia 23(3): 159-169.

Matsui T, Omasa K, Horie T (1999) Rapid swelling of pollen grains in response to floret opening unfolds anther locules in rice (*Oryza sativa* L.). Plant Production Science 2(3): 196-199.

McCubbin VA (1918) Dispersal distance of urediniospores of *Cronartium ribicola* as indicated by their rate of fall in still air. Phytopathological Notes 835-36.

Mitsumoto K, Yabusaki K, Aoyagi H (2009) Classification of pollen species using autofluorescence image analysis. Journal of bioscience and bioengineering 107(1): 90-94.

Niklas KJ (1982) Simulated and empiric wind pollination patterns of conifer ovulate cones. Proceedings of the National Academy of Sciences 79(2): 510-514.

Niklas KJ (1985) The aerodynamics of wind pollination. The Botanical Review 51(3): 328-386.

Norris WR (1995) A natural area inventory of Ames, Iowa. M.S. Thesis. Iowa State University. Available at: https://lib.dr.iastate.edu/rtd/313/ (Accessed: March 2021).

Ogden EC, Hayes JV, Raynor AGS (1969) Diurnal patterns of pollen emission in Ambrosia, Phleum, Zea, and Ricinus. American Journal of Botany 56(1): 16-21.

Paw U TK, Hotton C (1989) Optimum pollen and female receptor size for anemophily. American Journal of Botany 76: 445-453.

Pohl RW (1966) The grasses of Iowa. Iowa State J. Science 40: 341-566.

Radaeski JN, Bauermann SG, Pereira AB (2016) Poaceae pollen from Southern Brazil: distinguishing grasslands (campos) from forests by analyzing a diverse range of Poaceae species. Frontiers in Plant Science 7:1833.

Raynor GS, Ogden EC, Hayes JV (1972) Dispersion and deposition of corn pollen from experimental sources. Agronomy Journal 64(4): 420-427.

Rempe H (1937) Untersuchungen über die Verbreitung des Blütenstaubes durch die Luftströmungen. Planta 93-147.

Richardson P, Camper B (2019) Tangrams / heightmapper. Available at: https://tangrams.github.io/heightmapper/ (Accessed: October 2020)

Riest PC (1984) Introduction to Aerosol Science. Macmillan Publ. Co., New York and London.

Roussy AM, Kevan PG (2000) How accessible are receptive megastrobili to pollen? The example of Jack pine (Pinus banksiana). American Journal of Botany 87(2): 215-220.

Schwab CA (1971) Floral structure and embryology of *Diarrhena* (Gramineae). Ph.D Dissertation. Iowa State University. Available at: https://lib.dr.iastate.edu/rtd/4508/ (Accessed: March 2021).

Soreng RJ, Peterson PM, Romaschenko K, Davidse G, Zuloaga FO, Judziewicz EJ, Filgueiras TS, Davis JI, Morrone O (2015) A worldwide phylogenetic classification of the Poaceae (Gramineae). Journal of Systematics and Evolution 3(2):117-37.

Sosnoskie LM, Webster TM, Dales D, Rains GC, Grey TL, Culpepper AS (2009) Pollen grain size, density, and settling velocity for Palmer amaranth (Amaranthus palmeri). Weed Science 57(4): 404-409.

Stokes GG (1901) Mathematical and Physical Papers. Cambridge University Press. 3:60.

Strömberg CA (2011) Evolution of grasses and grassland ecosystems. Annual review of Earth and planetary sciences 39: 517-544.

Subba Reddi C, Raju NSN, Subba Rao MV (2010) Pollination and seed set in tropical wetland grasses. Nordic Journal of Botany 28(3): 354-365.

Subba Reddi CS, Reddi NS, Janaki BA (1988) Circadian patterns of pollen release in some species of Poaceae. Review of Palaeobotany and Palynology 54(1-2): 11-42.

Timerman D, Greene DF, Urzay J, Ackerman JD (2014) Turbulence-induced resonance vibrations cause pollen release in wind-pollinated *Plantago lanceolata* L. (Plantaginaceae). Journal of the Royal Society Interface 11(101): 20140866.

Timerman D, Barrett SC (2021) The biomechanics of pollen release: new perspectives on the evolution of wind pollination in angiosperms. Biological Reviews, 96(5): 2146-2163.

Van Hout R, Katz J (2004) A method for measuring the density of irregularly shaped biological aerosols such as pollen. Journal of Aerosol Science 35(11): 1369-1384.

Weather Underground (2020) Weather History for Des Moines, IA for the month of July 2020. Available at: https://www.wunderground.com/history/monthly/us/ia/des-moines/KDSM/date/2020-7 (Accessed: January 2021).

Whitehead DR (1969) Wind pollination in the angiosperms: evolutionary and environmental considerations. Evolution 23: 28-35.

Wodehouse RP (1935) Pollen grains. Their structure, identification and significance in science and medicine. *Pollen grains. Their structure, identification and significance in science and medicine.*